Am. J. Trop. Med. Hyg., 90(6), 2014, pp. 993–1002
doi:10.4269/ajtmh.13-0382

Endothelial Cell Permeability and Adherens Junction Disruption Induced by Junín Virus Infection

Heather M. Lander,* Ashley M. Grant, Thomas Albrecht, Terence Hill, and Clarence J. Peters
Departments of Pathology and Microbiology and Immunology, University of Texas Medical Branch, Galveston, Texas

Abstract. Junín virus (JUNV) is endemic to the fertile Pampas of Argentina, maintained in nature by the rodent host *Calomys musculinus*, and the causative agent of Argentine hemorrhagic fever (AHF), which is characterized by vascular dysfunction and fluid distribution abnormalities. Clinical as well as experimental studies implicate involvement of the endothelium in the pathogenesis of AHF, although little is known of its role. JUNV has been shown to result in productive infection of endothelial cells (ECs) *in vitro* with no visible cytopathic effects. In this study, we show that direct JUNV infection of primary human ECs results in increased vascular permeability as measured by electric cell substrate impedance sensing and transwell permeability assays. We also show that EC adherens junctions are disrupted during virus infection, which may provide insight into the role of the endothelium in the pathogenesis of AHF and possibly, other viral hemorrhagic fevers.

INTRODUCTION

Viral hemorrhagic fever (VHF) is a general term describing a severe illness characterized by fever, compromised hemostasis, and bleeding diathesis caused by members of four virus families: *Filoviridae*, *Bunyaviridae*, *Flaviviridae*, and *Arenaviridae*. The viruses that cause VHF have high mortality and morbidity, with very few readily available vaccines or treatments, and they pose threats as potential bioweapons. For these reasons, most are Centers for Disease Control and Prevention (CDC) category A agents and must be handled within biosafety level 4 (BSL4) laboratories.

Junín virus (JUNV) is a rodent-borne, enveloped RNA virus with an ambisense, bisegmented genome, which is classified in the Tacaribe serocomplex within the family *Arenaviridae*.[1] It is the etiologic agent of Argentine hemorrhagic fever (AHF), which was first described in 1955 in the Pampas of Argentina, where farm workers presented clinically with hemorrhagic, neurologic, and vascular manifestations. Like other arenaviruses, JUNV is carried by a specific reservoir (in this case, the rodent *Calomys musculinus* [dry land vesper mouse]). This reservoir specificity limits virus distribution to the general area of the Pampas, thereby posing the greatest risk for agricultural workers who can easily be infected by inhalation of aerosolized infectious excrement or contact with contaminated materials.

Vascular manifestations of AHF involve fluid distribution problems, vascular instability, thrombocytopenia, reduced serum complement activity, and hemorrhaging in the absence of overt endothelial cell cytopathology.[2] Neither disseminated intravascular coagulation (DIC) nor complement activation is typically observed in patients, although hemoconcentration and non-dependent periorbital edema are common, which generally indicates disease-related endothelial permeability.[3,4] AHF mortality ranges between 15% and 30%, although it can be reduced to 2% or less with convalescent plasma treatment.[2,3] Although the mechanisms of vascular instability during AHF are unknown, the paradigm is that mediators produced by virus-infected inflammatory cells contribute significantly.[5,6] However, endothelial cells are targeted to varying degrees by viruses causing VHFs,[7–10] and direct infection of these cells may also contribute to pathogenesis.

Little is known of the pathogenesis of JUNV or any of the other South American arenaviruses that cause VHFs, but clinical manifestations indicate a compromised endothelium with altered permeability. In general, the endothelium regulates permeability using transcellular and paracellular pathways to modulate the movement of protein and circulating cells from blood to tissues. Paracellular movement involves passage between cells through cell–cell junctions and therefore, was the focus of this study. The two major intercellular junctions identified in endothelial cells are tight junctions (TJs) and adherens junctions (AJs). Both are formed by the binding of transmembrane proteins to cytoplasmic proteins, which anchor them to the cytoskeleton. Although both types of junctions are involved in regulating vascular permeability, only AJs are ubiquitous throughout the vasculature, and there is substantial evidence that AJs and TJs are interconnected with AJs critical to TJ organization.[11–13] Furthermore, it has been shown that disruption of AJ alone is enough to dramatically increase permeability,[14] which contributes to pathogenesis of diseases, such as lead poisoning,[15] stroke,[16] sepsis,[17] and tumor metastasis.[18]

The major protein component of endothelial AJs is vascular endothelial cadherin (VE-cadherin), a transmembrane protein that binds to intracellular proteins[19,20] in the catenin family, namely α, β, and γ, and P120.[21] Figure 1 depicts these interactions.

Previous studies of JUNV in human umbilical vein endothelial cells (HUVECs) show that it productively infects the cells with no visible cytopathology.[7,22] It has also been shown in HUVECs that the virulent JUNV strain XJ decreases levels of released von Willebrand factor and increases production of intercellular adhesion molecule 1 (ICAM-1), vascular cellular adhesion molecule (VCAM), endothelial cell surface decay accelerating factor, endothelial nitric oxide synthase, and nitric oxide.[22] The aim of this study was to establish whether JUNV infection compromised HUVEC and human microvascular endothelial cells from the lung (HMVEC-L) monolayer integrity and investigate the direct effects of JUNV infection on AJ stability, protein expression, and cytokine levels.

*Address correspondence to Heather M. Lander, Sealy Center for Structural Biology and Molecular Biophysics, University of Texas Medical Branch, 301 University Boulevard, Galveston, TX 77555. E-mail: hmlander@utmb.edu

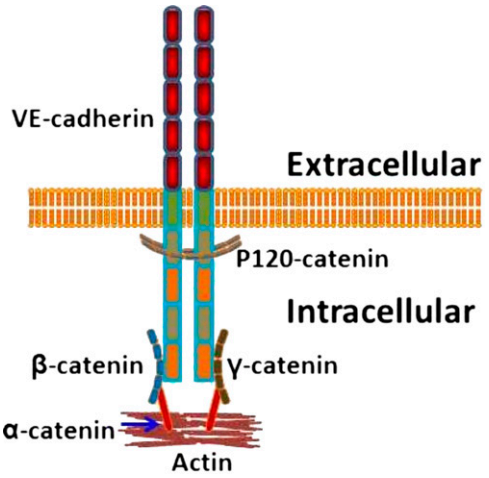

FIGURE 1. Diagramatic representation of the interactions between VE-cadherin and the catenins involved in AJs. P120-catenin binds to VE-cadherin near the membrane and plays an important role in regulating VE-cadherin turnover and junction integrity. β- and γ-catenin bind more distally and help secure the junction to the cytoskeleton through α-catenin. This illustration depicts the interactions that we were interested in for this study, but it does not show other known VE-cadherin associations, such as with vimentin, or any other associations that may occur within these junctions.

Our results show that, after infection with the virulent Romero strain of JUNV, HUVEC and HMVEC-L monolayers exhibited decreased electrical resistance, increased permeability to 70 kDa fluorescein isothiocyanate (FITC)-dextran, a reduction in VE-cadherin and P120-catenin levels, and alterations in the actin cytoskeleton. We also found that HUVEC and HMVEC-L monolayers infected with JUNV expressed increased levels of monocyte chemoattractant protein-1 (MCP-1) and interleukin-6 (IL-6), with no evidence of increased vascular endothelial growth factor (VEGF) production or Src kinase activation. These data are the first evidence that endothelial cell responses to direct JUNV infection contribute to disorganization of endothelial cell AJs, which could play a major role in the pathogenesis of JUNV.

MATERIALS AND METHODS

Cell culture. Primary single-donor HUVEC and HMVEC-L (Lonza, Walkerville, MD) were cultured in endothelial cell basal medium bullet kits (Lonza) containing 20% fetal bovine serum (FBS; Gibco, Aukland, New Zealand) supplemented with L-glutamine and antibiotics on 100-mm plates coated with type I rat tail collagen (Millipore/Upstate, Temecula, CA) at 10 μg/cm^2. Cells were used at passages three through seven in all experiments. Cells were infected with JUNV, Romero, or Candid#1 strain at a multiplicity of infection (MOI) of four unless otherwise indicated. Vero E6 cells were cultured in Dulbecco's modified Eagle medium (DMEM) plus 10% FBS supplemented with L-glutamine and antibiotics/antimycotics (Gibco).

Virus. JUNV Candid#1 was initially developed as a human vaccine.[23] We acquired it from Robert Tesh (University of Texas Medical Branch, Galveston, TX) after one passage in suckling mice. It was passaged again in Vero E6 cells at 35°C, which generated the highest stock titers, to create a working stock for infections. JUNV strain Romero was obtained from Mike Holbrook (University of Texas Medical Branch, Galveston, TX). The virus underwent four passages in Vero cells to generate working stocks. All virulent virus work was performed in the University of Texas Medical Branch BSL4 facility according to institutional health and safety guidelines.

Reagents and antibodies. The following antibodies were used: goat anti–β-catenin (E-17; Santa Cruz Biotechnologies, Santa Cruz, CA), mouse anti–β-catenin (E-5; Santa Cruz), goat anti–VE-cadherin (C-19; Santa Cruz), and mouse anti–platelet/endothelial cell adhesion molecule-1 (PECAM-1) (E-8; Santa Cruz).

Viral infection of cells. Cells were seeded at 3.3 × 10^4 cells/cm^2 and allowed to reach 100% confluency, which was defined as the point at which the monolayer barrier function reached stable levels as determined by electric cell substrate impedance sensing (ECIS). When seeded at this density, the monolayers needed 108 hours to reach confluency. Within 6 hours of reaching confluency, monolayers were infected with either Candid#1 or Romero at MOI = 4, or they were mock-infected. Because virus stocks were generated in Vero cells and not purified, mock infections were done with culture-matched Vero cell supernatant.

ECIS. The ECIS system model 1600R and 8W10E+ arrays (Applied Biophysics Inc, Troy, NY) were used for these studies. The array chambers were coated with 10 μg/cm^2 type I rat tail collagen for 30 minutes at 37°C. HUVEC and HMVEC-L cells were seeded at a density of 3.3 × 10^4 cells/cm^2 and infected with JUNV or mock-infected at 108 hours post-seeding. Resistance, capacitance, and impedance information was collected continuously for 4 days post-infection. Each experiment had six replicates and was repeated three times.

Transwell permeability assays. HUVECs and HMVEC-Ls were seeded at passage five at a density of 3.3 × 10^4 cells/cm^2 on collagen-coated (10 μg/cm^2) Transwell polycarbonate filters (pore size = 0.4 μm, exposed area = 1 cm^2; Costar, Brumath, France). JUNV infection was performed at 108 hours post-seeding. FITC-dextran (molecular mass of 70 kDa; Sigma) was used as an index of macromolecular diffusion. After infection with JUNV or mock infection, 1 mg/mL FITC-dextran in HUVEC medium was added to the upper chambers of the Transwell system; 100-μL samples were taken from the lower chamber at 24-hour intervals, and the same volume of HUVEC medium was replaced in this chamber to prevent fluid movement caused by hydrostatic pressure. The fluorescence was measured with a spectrophotometer (Fluoroskan Ascent; Thermo-Scientific, Waltham, MA) using 480 and 520 nm as the excitation and emission wavelengths, respectively. The quantities of all albumin dextrans were estimated using a standardization curve.

Immunocytochemistry. HUVECs and HMVEC-Ls were seeded at 3.3 × 10^4 cells/cm^2 on collagen-coated Permanox chamber slides (Nalge Nunc International, Rochester, NY) and infected with JUNV at 108 hours post-seeding. Chamber slides were fixed in 4% paraformaldehyde in phosphate-buffered saline (PBS) for 10 minutes at room temperature, and then permeabilized in 0.2% TritonX-100 in PBS for 5 minutes at room temperature. Alexa Fluor 488- and Alexa Fluor 594-labeled (both diluted at 1:500; Molecular Probes, Leyden, The Netherlands) secondary antibodies were used for fluorescence detection. Slides were mounted

using Prolong Gold antifade reagent with 4′,6-diamidino-2-phenylindole (DAPI; Invitrogen, Eugene, OR) to stain for nuclei. Confocal images were acquired using Zeiss LSM 510 w.s. software on a Zeiss Axiovert 200M inverted microscope (Carl Zeiss, Oberkochen, Germany).

Cytokine analysis. Supernatant samples from HUVEC and HMVEC-L monolayers infected with JUNV or mock-infected were collected at 24-hour time points for 5 days post-infection and analyzed by Bioplex (Bio-Rad, Hercules, CA), VeriKine enzyme-linked immunosorbent assays (ELISAs; 41100-1 or 41410-1; PBL, Piscataway, NJ), or an interferon bioassay. The Bioplex and VeriKine assays were performed according to the manufacturer's protocols. For the interferon bioassay, Vero cells were seeded in 96-well plates at 1.5×10^5 cells/mL and incubated at 37°C. After 24 hours, the plates were decanted, and 110 μL Eagle's minimal essential medium (EMEM) with 2% FBS were added to each well; 50 μL each cell supernatant were added to the wells in duplicate and serially diluted to 1:3. The plates were incubated for 24 hours at 37°C, after which time they were decanted and washed three times with Hanks' balanced salt solution (HBSS). After the last wash, 25 μL Sindbis virus were added to each well, except for the cell controls, which received 25 μL EMEM with 2% FBS. Plates were incubated for 1 hour at 37°C and then, decanted; 100 μL methylcellulose were added. After another 24 hours of incubation at 37°C, the plates were stained with crystal violet, and plaques were counted.

RESULTS

Infection with JUNV decreases HUVEC and HMVEC-L monolayer barrier function. To determine whether JUNV infection disrupts endothelial cell monolayer barrier function, ECIS was used to evaluate virus-infected HUVEC and HMVEC-L monolayer barrier integrity compared with mock-infected controls. Confluent monolayers of HUVECs or HMVEC-Ls were infected with either JUNV Romero or Candid#1 at MOI = 4 or mock-infected, and they were monitored continuously by the ECIS system. In this system, as the monolayer reaches confluency, cell membranes impede the electrical current unless there are gaps through which the current can move. Pre-infection resistance levels were used to verify that confluency was reached and maintained and that the cells exhibited normal low levels of resistance fluctuations. Decreased resistance indicated reduced monolayer barrier integrity. To control for the presence of permeability-inducing mediators in the unpurified viral stocks, all mock infections were performed using culture-matched uninfected Vero cell supernatant. As shown in Figure 2, at approximately 60 hours post-infection, electrical resistance of both the JUNV Romero- and Candid#1-infected HUVEC (Figure 2A) and HMVEC-L (Figure 2B) monolayers decreased relative to mock-infected cells. No visible cytopathology of infected monolayers was seen using phase contrast microscopy (Figure 2, insets), and productive infection and absence of cytotoxicity for each study were verified by using supernatant samples to generate growth curves (data not shown).

γ-Irradiation of JUNV prevents the virus-induced decrease in electrical resistance in HUVEC and HMVEC-L monolayers. To determine if viral replication and productive cellular infection are necessary for the observed increase in permeability, γ-irradiated virus was used to infect the cells. Virus stocks were subjected to 5 M Rad γ-irradiation, after which no virus growth could be detected. We report no decrease in electrical resistance on treatment with killed JUNV in either endothelial cell type tested (Figure 2). Also, we did not find increased permeability or surface expression changes in AJ proteins with γ-irradiated JUNV (Figures 3–5). Because this irradiated JUNV did not decrease electrical resistance or increase permeability and because it has been shown that irradiation does not significantly affect proinflammatory small molecules,[24] this γ-inactivated virus also served to further control for virus propagation in Vero cells.

Infection with JUNV increases HUVEC and HMVEC-L monolayer permeability to 70 kDa FITC-dextran. To establish the physiological relevance of the ECIS data, Transwell permeability assays were performed to determine if the drop in electrical resistance coincided with increased permeability of the endothelial monolayers to 70 kDa FITC-dextran. Confluent monolayers of HUVECs or HMVEC-Ls were infected with JUNV or mock-infected with Vero cell culture supernatant. After infection, 70 kDa FITC-dextran was added to evaluate whether molecules that were approximately the size of albumin would be able to move through the monolayer during JUNV infection. Virus infection significantly increased the amount of 70 kDa FITC-dextran allowed to pass through HUVEC and HMVEC-L monolayers (Figure 3A) compared with mock-infected cells (Figure 3B).

JUNV infection coincides with decreased VE-cadherin and P120 immunofluorescence. AJs are critical in maintaining endothelial barrier integrity, and VE-cadherin is the main protein component of these junctions. Under normal physiological conditions, VE-cadherin is degraded and resynthesized as cellular and tissue requirements demand. Immunofluorescent staining, of JUNV-infected HUVEC and HMVEC-L monolayers was used to determine whether JUNV infection altered the levels of VE-cadherin. As early as 24 hours post-infection, virus-infected cells showed decreased VE-cadherin (Figure 4), and as viral antigen expression increased over time, there was a corresponding decrease in VE-cadherin expression until levels were nearly below the level of detection at 96 hours post-infection. A loss of VE-cadherin was also seen in non-infected cells that bordered infected cells but not cells that were not infected and not bordering infected cells. This result contrasted with mock-infected cells, in which VE-cadherin expression remained strong throughout the time course. Figure 4C and D shows Western blot data confirming the immunostaining results.

P120-catenin is also a critical component of AJs and has been shown to play a role in vascular permeability during metastasis of certain tumor types.[25] It binds to the juxtamembrane domain of VE-cadherin and has been shown to modulate intracellular levels of VE-cadherin by regulating clathrin-mediated endocytosis.[26,27] In this study, P120 staining was decreased in cells that were infected or adjacent to cells infected with either JUNV Romero or Candid#1, and this decrease was confirmed by Western blotting (Figure 5).

JUNV infection does not induce VEGF production or Src activity. VEGF and phosphorylated cSrc (tyr416) levels were measured in supernatants of cells either virus- or mock-infected to determine if the observed changes in

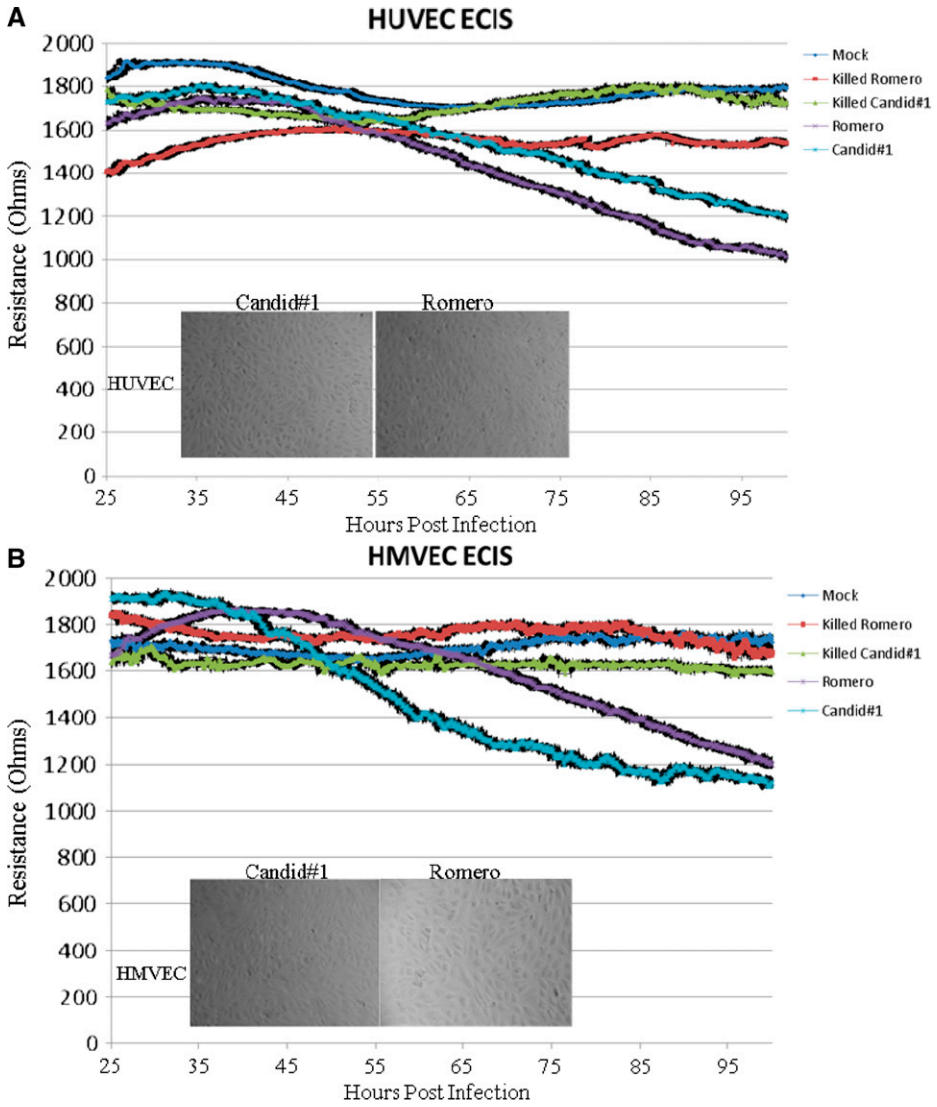

FIGURE 2. ECIS. Cells were seeded onto collagen-coated gold electrode arrays and allowed to reach confluence (108 hours post-seeding). Monolayers were then infected with either mock, killed Romero, killed Candid#1, Romero, or Candid#1 at MOI = 4, and impedance measurements were made continuously for 100 hours. Live JUNV infection decreased HUVEC and HMVEC-L monolayer electrical resistance. (**A**) HUVECs or (**B**) HMVEC-Ls infected with JUNV Romero or Candid#1 show decreased electrical resistance beginning at approximately 60 hours post-infection. Mock and killed virus data show no decrease in electrical resistance. Data shown are the mean ± SD of three independent experiments. Insets show phase-contrast images of cell monolayers, indicating no visible cytopathology during experimental JUNV infections in either (**A**) HUVECs or (**B**) HMVEC-Ls.

permeability and AJ architecture involved up-regulation of VEGF or cSrc activity. We found no increase in either VEGF levels or phosphorylated cSrc in either HUVECs or HMVEC-Ls infected with JUNV (data not shown).

JUNV infection increases HUVEC and HMVEC-L production of IL-6 and MCP-1. Because cytokines are important in mediating vascular permeability, levels of HUVEC and HMVEC-L cytokine production during JUNV infection were measured. In addition to the classical permeability-inducing cytokines, tumor necrosis factor-α (TNF-α), interferon-γ (IFN-γ), IL-6, MCP-1, IL-1b, IL-2, IL-4, IL-5, IL-7, IL-8, IL-10, IL-12(p70), IL-13, IL-17, granulocyte colony-stimulating factor (G-CSF), granulocyte-macrophage colony-stimulating factor (GM-CSF), IFN-α, and IFN-β were measured. The only cytokines that were increased, relative to mock infection, were IL-6 and MCP-1 (Figure 6).

DISCUSSION

Clinical manifestations of AHF indicate vascular dysregulation with increased vascular permeability in the absence of overt endothelial damage. Patients exhibit thrombocytopenia, leucopenia, proteinuria, and fluid distribution problems. Vomiting and dehydration can cause a rising hematocrit, which indicates a decrease in plasma volume rather than an increase in the number of red blood cells, but even hospitalized patients receiving fluid replacement experience hemoconcentration. Hemorrhage occurs, and clinically, it is usually more severe than immune thrombocytopenic purpura or other non-VHF conditions at similar levels of thrombocytopenia. These observations implicate an endothelium that, although not visibly damaged, is altered enough to initiate a permeability increase that, when combined with other

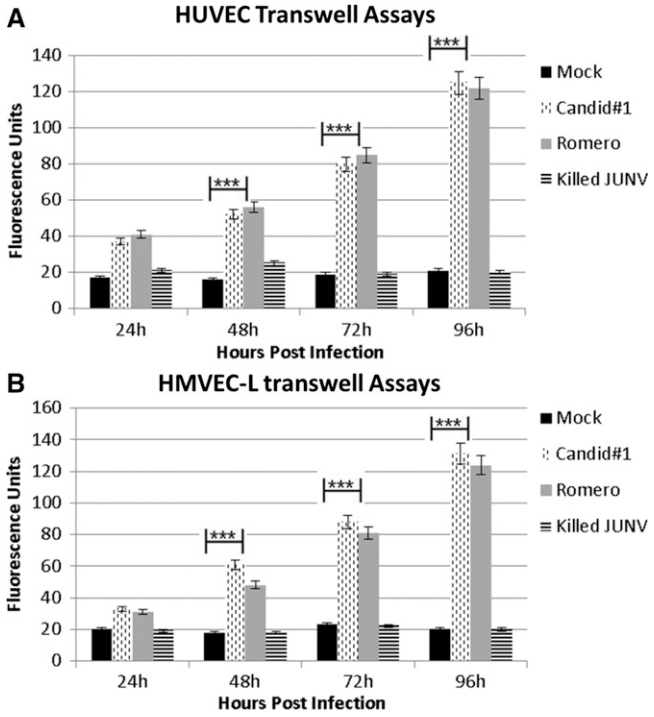

FIGURE 3. Transwell permeability assay. Cells were seeded onto Transwell inserts and infected with JUNV Romero, Candid#1, or γ-irradiated JUNV at MOI = 4 or mock-infected. Samples were taken every 24 hours for 5 days. (**A**) HUVECs or (**B**) HMVEC-Ls infected with JUNV show an extremely significant increased permeability to 70 kDa FITC-dextran in the absence of visible cytopathology. ***$P < 0.0001$ by paired t test. Data shown are the mean ± SD of three independent experiments.

physiological factors during infection, may contribute to development of disease.

The presence of a vascular syndrome in the absence of overt vascular damage is not surprising considering that other viral infections result in altered cellular processes without overt cellular injury. For example, lymphocytic choriomeningitis virus, another arenavirus, alters growth hormone levels in the pituitaries of CH3/ST mice while leaving housekeeping functions undisturbed.[28,29] For this reason, we used a cell culture model to establish the role of direct JUNV infection of endothelial cells in virus-induced vascular dysregulation. Our results show that direct infection with either JUNV strain decreases endothelial monolayer barrier function (Figure 2) and increases endothelial monolayer permeability to FITC-dextran in the absence of visible cytopathology (Figure 3). We also found that this dysfunction is associated with changes in AJ stability, including decreases in VE-cadherin (Figure 4) and P120-catenin (Figure 5). Taken together, these findings indicate that direct JUNV infection contributes to endothelial cell function alterations *in vitro*, resulting in increased endothelial dysfunction and decreased endothelial barrier integrity.

Our JUNV model is not the only system in which VE-cadherin levels play a role in permeability regulation. There is extensive data that VE-cadherin functions in numerous ways to dynamically regulate vascular permeability under normal physiologic processes, such as angiogenesis and wound healing, but also, in pathogenic situations.[30,31] Myriad pathways are involved, and each pathway is regulated independently. For example, TNF-α activates Fyn during sepsis, which results in the opening of the AJ, contributing to multiorgan failure,[17] and when P120-catenin mismanages the turnover of VE-cadherin, the permeability required for some kinds of tumor metastasis can occur.[32] VEGF signaling and Src kinase activation are also involved in many disease processes involving AJ disruption and inappropriate permeability, such as lead poisoning[15] and myocardial infarction.[15,33] It has also been shown that patients with dengue hemorrhagic fever have higher serum levels of VEGF and that Andes hantavirus-induced endothelial permeability is related to VEGFR2 signaling by Src; it can be decreased through Src and VEGFR2 inhibitors.[34–36] However, we found no evidence in our JUNV model that disruption of AJs is through VEGFR2/Src-mediated signaling. VEGF signaling occurs very quickly and can be missed if it reverses before sample collection, but in this system of productive infection, VEGF signaling and subsequent Src activation would have been ongoing and detectable at the chosen time points. Rather than VEGF/Src, this study indicates that P120-mediated VE-cadherin decrease is more likely the mechanism of AJ disruption in response to JUNV infection.[37] In the event of insufficient P120 levels to prevent clathrin-mediated endocytosis and degradation of VE-cadherin, the endothelial AJ would be compromised. Therefore, the next logical step in identifying the mechanism of this permeability induction is to specifically investigate the effects of JUNV infection and cytokine release on P120 transcription, degradation, and signaling.

In an effort to improve our understanding of the endothelial cell response to JUNV infection, we investigated cytokine levels and found increased levels of IL-6 and MCP-1. In the endothelium, IL-6 is a known inducer of angiogenesis and can cause endothelial permeability as well as induce the production of MCP-1.[38–40] MCP-1 plays a role in angiogenesis and wound repair, has been shown to induce permeability, and is found significantly increased in dengue hemorrhagic fever patients as well as human endothelial cells infected with *Rickettsia in vitro*.[41,42] Because both MCP-1 and IL-6 have been shown to function synergistically to increase vascular inflammation,[43] it is possible that they function together during JUNV infection to induce signaling that leads to AJ dysregulation with subsequent permeability increases. The biphasic nature of this increased expression is not completely unexpected, because it has been seen with IL-6 and MCP-1 in other pathogenic circumstances, such as irradiation and a mouse model of otitis media with effusion.[44,45] This result suggests an initial increase that induces intracellular signaling events that lay the groundwork for pathogenesis as well as initiate additional cytokine expression. This result is also consistent with previous reports that patients with AHF showed increased circulating levels of IL-6.[6] In addition, because we are only able to visualize these changes in cells infected with JUNV or bordered by infected cells, the mechanism of action on the AJ proteins seems to involve an intracellular cascade rather than intercellular signaling or paracrine cytokine effect. It is possible that cellular infection with JUNV initiates signaling that triggers IL-6 or MCP-1 synthesis with a subsequent loss of P120-catenin, leading to the loss of VE-cadherin. Any VE-cadherin molecules on adjacent, uninfected cells would then lose their homophilic junctional partners, and the loss would initiate degradation of those newly unanchored

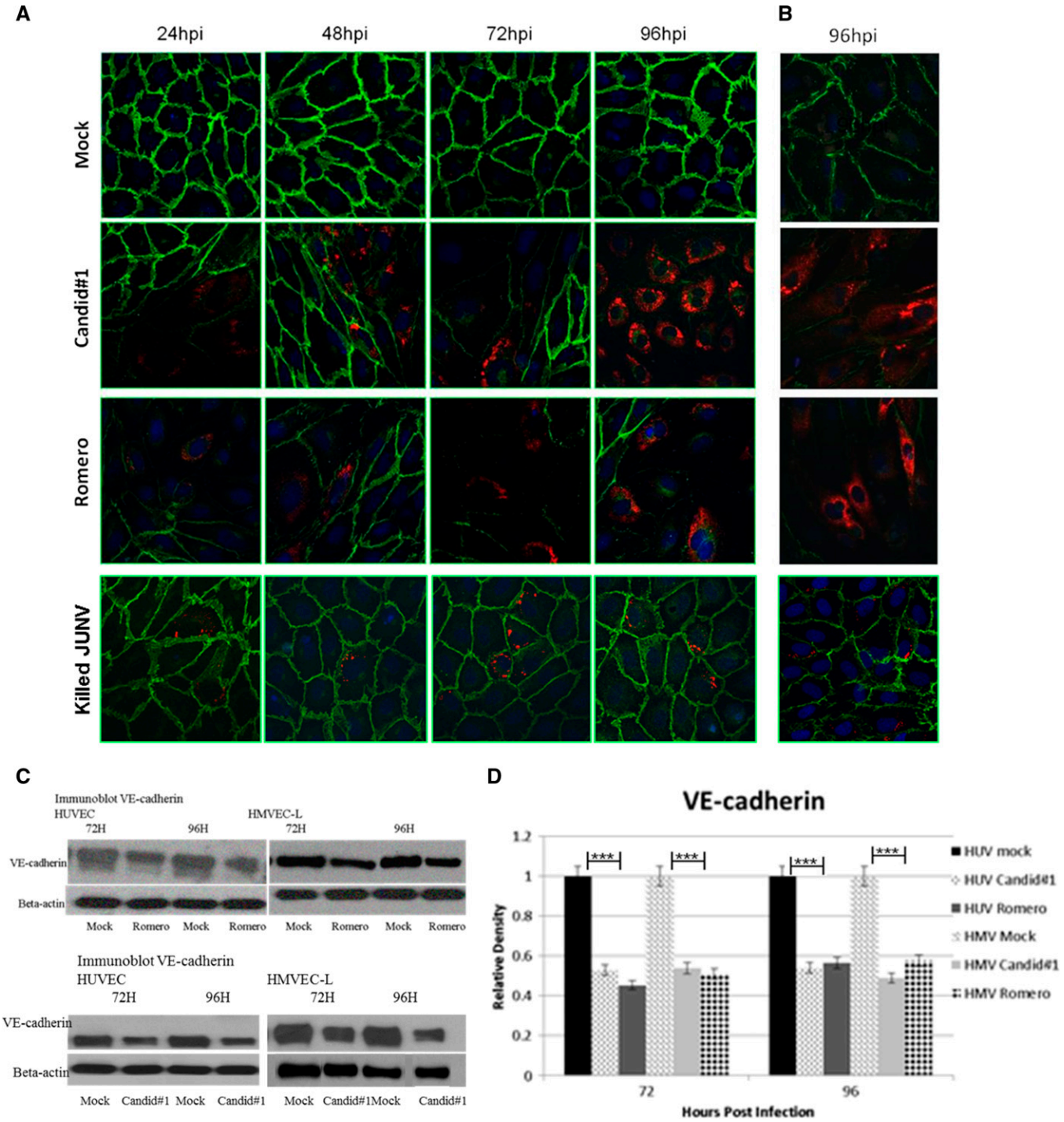

FIGURE 4. Immunocytochemistry of VE-cadherin. JUNV infection greatly decreases VE-cadherin staining in (**A**) HUVECs and (**B**) HMVEC-Ls, but γ-irradiated JUNV does not alter VE-cadherin staining. Cell monolayers were infected with JUNV Romero, Candid#1, or γ-irradiated JV at MOI = 4 or mock-infected; then, they were fixed at 24-hour intervals up to 96 hours. Green, Alexa Fluor 488 (VE-cadherin); red, Alexa Fluor 594 (Junin virus); blue, DAPI. All images are 40× magnification. All time points for HUVECs are shown, and a representative time point is shown for HMVEC-Ls. hpi = hours post-infection. (**C**) Western blots and (**D**) Image J analysis of Western blot density. The relative density is normalized to β-actin, and the mock is set as 1.0. Values are averages from three independent experiments. Data shown are the mean ± SD. A Student's *t* test was used for statistical analysis. ***$P < 0.001$.

VE-cadherin molecules. It may also critically impair junctional associations with the actin network, which has been shown to interact with JUNV (an interaction necessary for viral entry and replication).[46,47] Future mechanistic studies must look closely at the role that JUNV–actin interactions might play in compromised endothelial function. Using reverse genetics to selectively express viral gene products during infection would provide valuable information regarding which viral components are critical in this regard. In addition, an *in vivo* system is needed to more closely investigate the role of IL-6

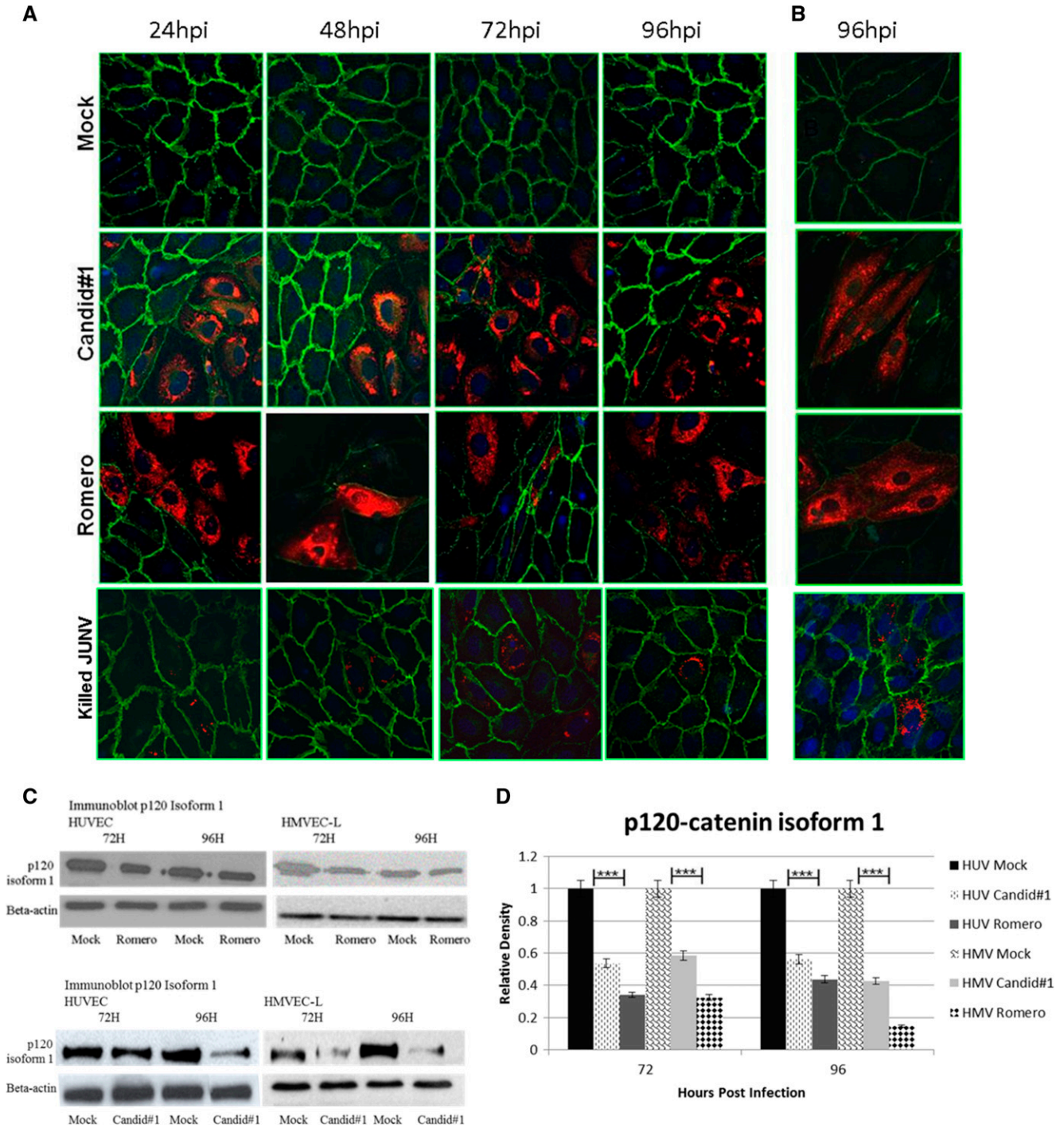

FIGURE 5. Immunocytochemistry of P120-catenin. JUNV infection greatly decreases P120-catenin staining in (**A**) HUVECs and (**B**) HMVEC-Ls, but γ-irradiated JUNV does not alter P120-catenin staining. Cell monolayers were infected with JUNV Romero, Candid#1, or γ-irradiated JUNV at MOI = 4 or mock-infected; then, they were fixed at 24-hour intervals up to 96 hours. Green, Alexa Fluor 488 (P120-catenin); red, Alexa Fluor 594 (Junin virus); blue, DAPI. All images are 40× magnification. All time points for HUVECs are shown, and a representative time point is shown for HMVEC-Ls. hpi = hours post-infection. (**C**) Western blots and (**D**) Image J analysis of Western blot density. The relative density is normalized to β-actin, and the mock is set as 1.0. Values are averages from three independent experiments. Data shown are the mean ± SD. A Student's *t* test was used for statistical analysis. ***$P < 0.001$.

and MCP-1 on signaling pathways and P120 levels during JUNV infection.

Circulating IFNs have also been previously shown to play an important role in arenavirus-mediated diseases, with increased levels correlated to increased disease severity[5,48–50] In this study, we were unable to detect IFN-α, -β, or -γ in human endothelial cells infected with JUNV. Although this result indicates that the cells themselves are not responding to infection with JUNV by expressing IFN, we cannot rule out the influence of immune cells and other intercellular signaling

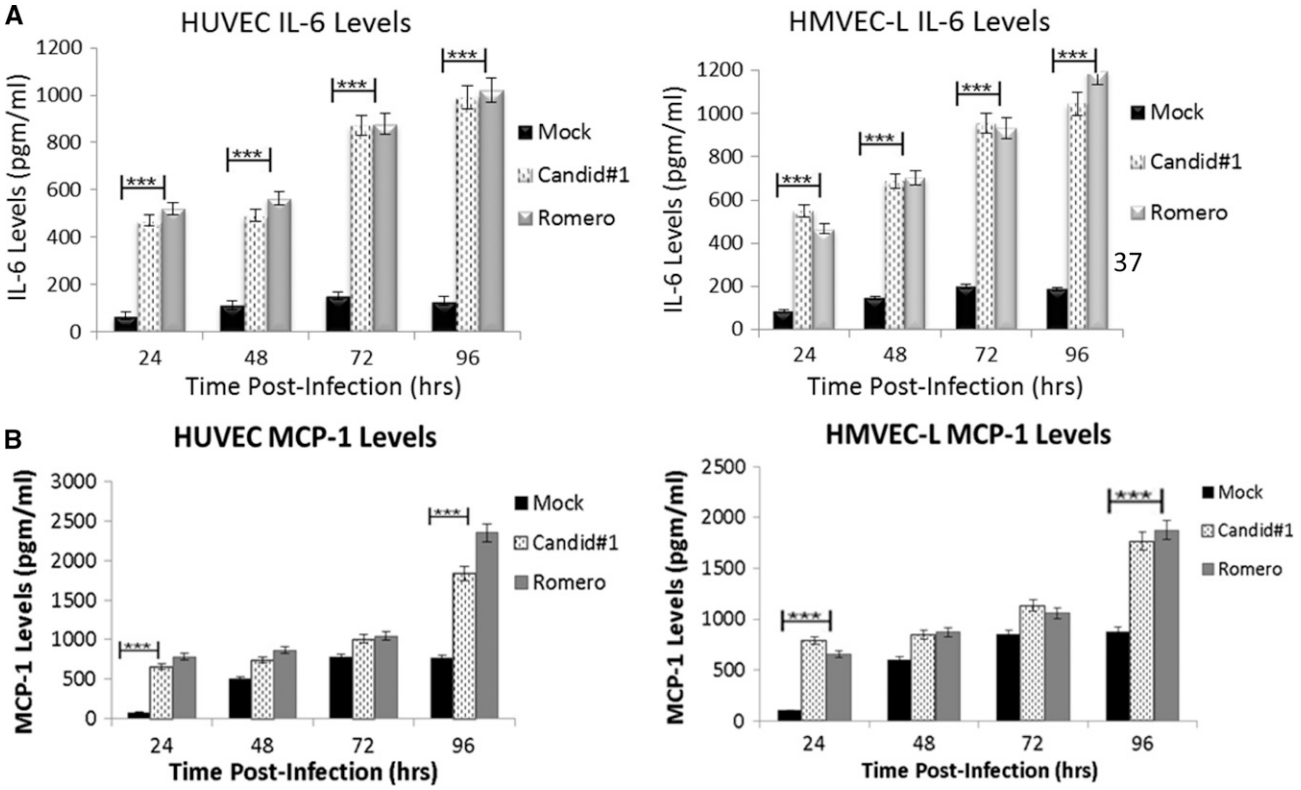

FIGURE 6. Cytokine analysis. HUVEC and HMVEC-L supernatants were analyzed for cytokine levels during infection with JUNV Romero or Candid#1 at MOI = 4 or mock-infected. Supernatant samples were taken every 24 hours post-infection and subjected to Bioplex cytokine analysis, ELISA, or the IFN bioassay. The only cytokines measured that were changed compared with mock-infected cells were (**A**) IL-6 and (**B**) MCP1, which were both significantly increased compared with mock-infected cells. Data shown are the mean ± SD. Data is extremely significant by a two-way repeated measure analysis of variance (ANOVA) test. ***P value < 0.0001.

events that occur *in vivo* in response to JUNV infection; *in vivo* studies will be critical in addressing this issue.

Notably and unexpectedly, when the experiments were performed using the attenuated strain of JUNV, Candid#1, the results were indistinguishable from those results seen with the virulent Romero strain. This finding clearly indicates that the mechanism of attenuation of Candid#1 does not involve inhibition of the mechanism of endothelial cell disruption and permeability induction. Instead, it seems that Candid#1 must not be able to disseminate and/or replicate to the same degree as the wild-type, virulent Romero strain. Perhaps it involves some level of temperature sensitivity or a reduced ability of the virus to evade immune responses. Recently, a study to rescue JUNV strains from cloned cDNAs suggests that Candid#1 does, in fact, replicate more slowly than Romero.[51] Of course, in this *in vitro* system, there are no immune responses; therefore, *in vivo* studies are needed to evaluate the effects of immune responses to Candid#1 replication and dissemination and more clearly elucidate the mechanism of attenuation. Although it might also call into question whether the observed endothelial response to JUNV infection is a general response to viral infection rather than a specific response to JUNV, the distinction, for the purposes of investigating pathogenesis, is irrelevant. Regardless of the specificity of this response, it would contribute to disease progression and must be included in the assessment of pathogenesis and development of potential prophylactic or therapeutic measures.

Although our study indicates the involvement of direct JUNV infection in the pathogenesis of AHF, we must not disregard the role of other key components that are present *in vivo* and cannot be evaluated using cell culture models. In particular, inflammatory cells, whether infected or recruited, and the biochemical compounds that they produce most certainly affect pathogenesis and disease progression. Finally, the extracellular matrix is a vital and dynamic component of the vasculature that responds to both endothelial signaling and endothelial damage to facilitate wound healing and angiogenesis. The role of this matrix during JUNV infection and the development of the vascular syndrome remains unknown and requires additional inquiry.[52]

Members of the Arenaviridae, Bunyaviridae, Flaviviridae, and Filoviridae all mediate VHF, and clearly, it is possible that there are different pathogenic mechanisms for the development of disease, because the interaction of each virus with the vasculature is unique. For example, TNF-α and endothelial cell damage play a role in filovirus infections.[53] Some hantaviruses seem to increase endothelial permeability through AJs by VEGF, whereas others may also involve immune mediation by IFN-γ.[54] MCP-1 has been shown to increase permeability of the endothelium in dengue hemorrhagic fever but is induced in monocytes and lymphocytes rather than within the endothelium.[34,55] Therefore, we are not surprised that our cell culture system indicates that JUNV may use a different pathway compared with other VHFs to increase endothelial permeability, and we believe

that this study indicates the potential role of synergy between endothelial cell infection and other host responses in disease development during AHF.

Received June 27, 2013. Accepted for publication November 19, 2013.

Published online April 7, 2014.

Acknowledgments: The authors thank Dr. Robert Tesh (University of Texas Medical Branch) for providing the anti-Junin mouse ascitic fluid, Dr. Mike Holbrook (University of Texas Medical Branch) for providing the Junin Romero strain, and Drs. Nadya Yun (University of Texas Medical Branch) and Slobodan Paessler (University of Texas Medical Branch) for providing valuable technical help in the BSL4. Dr. Sara M. Weis at the University of California San Diego (UCSD) Moore Cancer Center provided invaluable technical advice and insight. We also thank Dr. Mike Woods for technical advice, Jamal Saada for the original illustration, Dr. Eric Mossel (Centers for Disease Control and Prevention) for useful discussions and comments on the manuscript, and Dr. Alan Barrett (University of Texas Medical Branch) for help with manuscript editing.

Financial support: This work was supported by the Department of Pathology, University of Texas Medical Branch; National Institutes of Health Biodefense Training Grant T32 AI060549; and the John Sealy Foundation, University of Texas Medical Branch.

Authors' addresses: Heather M. Lander, Sealy Center for Structural Biology and Molecular Biophysics, University of Texas Medical Branch, Galveston, TX, E-mail: hmlander@utmb.edu. Ashley M. Grant, United States Department of Defense, Washington, DC, E-mail: ashleymariegrant@gmail.com. Thomas Albrecht, Department of Microbiology and Immunology, University of Texas Medical Branch, Galveston, TX, E-mail: talbrecht731@yahoo.com. Terence Hill, Department of Microbiology and Immunology, University of Texas Medical Branch, Galveston, TX, E-mail: tehill@utmb.edu. Clarence J. Peters, Department of Microbiology and Immunology, University of Texas Medical Branch, Galveston, TX, E-mail: cjpeters@utmb.edu.

REFERENCES

1. Bushar G, Sagripanti JL, 1997. Molecular characteristics of Junin virus. *J Virol Methods 63:* 27–35.
2. de Bracco MME, Rimoldi MT, Cossio PM, Rabinovich A, Maiztegui JI, Carballal G, Arana RM, 1978. Argentine hemorrhagic fever. *N Engl J Med 299:* 216–221.
3. Molteni HD, Guarinos HC, Petrillo CO, Jaschek F, 1961. Clinico-statistical study of 338 patients with epidemic hemorrhagic fever in the northwest of the province of Buenos Aires. *Sem Med 118:* 839–855.
4. Nguyen TH, Nguyen TL, Lei HY, Lin YS, Le BL, Huang KJ, Lin CF, Do QH, Vu TQ, Lam TM, Yeh TM, Huang JH, Liu CC, Halstead SB, 2006. Volume replacement in infants with dengue hemorrhagic fever/dengue shock syndrome. *Am J Trop Med Hyg 74:* 684–691.
5. Levis SC, Saavedra MC, Ceccoli C, Falcoff E, Feuillade MR, Enria DA, Maiztegui JI, Falcoff R, 1984. Endogenous interferon in Argentine hemorrhagic fever. *J Infect Dis 149:* 428–433.
6. Marta RF, Montero VS, Hack CE, Sturk A, Maiztegui JI, Molinas FC, 1999. Proinflammatory cytokines and elastase-alpha-1-antitrypsin in Argentine hemorrhagic fever. *Am J Trop Med Hyg 60:* 85–89.
7. Andrews BS, Theofilopoulos AN, Peters CJ, Loskutoff DJ, Brandt WE, Dixon FJ, 1978. Replication of dengue and junin viruses in cultured rabbit and human endothelial cells. *Infect Immun 20:* 776–781.
8. Lukashevich IS, Maryankova R, Vladyko AS, Nashkevich N, Koleda S, Djavani M, Horejsh D, Voitenok NN, Salvato MS, 1999. Lassa and Mopeia virus replication in human monocytes/macrophages and in endothelial cells: different effects on IL-8 and TNF-alpha gene expression. *J Med Virol 59:* 552–560.
9. Hippenstiel S, Suttorp N, 2003. Interaction of pathogens with the endothelium. *Thromb Haemost 89:* 18–24.
10. Peters CJ, Zaki SR, 2002. Role of the endothelium in viral hemorrhagic fevers. *Crit Care Med 30:* S268–S273.
11. Breviario F, Caveda L, Corada M, Martin-Padura I, Navarro P, Golay J, Introna M, Gulino D, Lampugnani MG, Dejana E, 1995. Functional properties of human vascular endothelial cadherin (7B4/cadherin-5), an endothelium-specific cadherin. *Arterioscler Thromb Vasc Biol 15:* 1229–1239.
12. Dejana E, Orsenigo F, Lampugnani MG, 2008. The role of adherens junctions and VE-cadherin in the control of vascular permeability. *J Cell Sci 121:* 2115–2122.
13. Taddei A, Giampietro C, Conti A, Orsenigo F, Breviario F, Pirazzoli V, Potente M, Daly C, Dimmeler S, Dejana E, 2008. Endothelial adherens junctions control tight junctions by VE-cadherin-mediated upregulation of claudin-5. *Nat Cell Biol 10:* 923–934.
14. Gao X, Kouklis P, Xu N, Minshall RD, Sandoval R, Vogel SM, Malik AB, 2000. Reversibility of increased microvessel permeability in response to VE-cadherin disassembly. *Am J Physiol Lung Cell Mol Physiol 279:* L1218–L1225.
15. Hossain MA, Russell JC, Miknyoczki S, Ruggeri B, Lal B, Laterra J, 2004. Vascular endothelial growth factor mediates vasogenic edema in acute lead encephalopathy. *Ann Neurol 55:* 660–667.
16. Paul R, Zhang ZG, Eliceiri BP, Jiang Q, Boccia AD, Zhang RL, Chopp M, Cheresh DA, 2001. Src deficiency or blockade of Src activity in mice provides cerebral protection following stroke. *Nat Med 7:* 222–227.
17. Angelini DJ, Hyun SW, Grigoryev DN, Garg P, Gong P, Singh IS, Passaniti A, Hasday JD, Goldblum SE, 2006. TNF-alpha increases tyrosine phosphorylation of vascular endothelial cadherin and opens the paracellular pathway through fyn activation in human lung endothelia. *Am J Physiol Lung Cell Mol Physiol 291:* L1232–L1245.
18. Cheung LW, Leung PC, Wong AS, 2010. Cadherin switching and activation of p120 catenin signaling are mediators of gonadotropin-releasing hormone to promote tumor cell migration and invasion in ovarian cancer. *Oncogene 29:* 2427–2440.
19. Lampugnani MG, 2010. Endothelial adherens junctions and the actin cytoskeleton: an 'infinity net'? *J Biol 9:* 16.
20. Harris TJ, Tepass U, 2010. Adherens junctions: from molecules to morphogenesis. *Nat Rev Mol Cell Biol 11:* 502–514.
21. Vincent PA, Xiao K, Buckley KM, Kowalczyk AP, 2004. VE-cadherin: adhesion at arm's length. *Am J Physiol Cell Physiol 286:* C987–C997.
22. Gomez RM, Pozner RG, Lazzari MA, D'Atri LP, Negrotto S, Chudzinski-Tavassi AM, Berria MI, Schattner M, 2003. Endothelial cell function alteration after Junin virus infection. *Thromb Haemost 90:* 326–333.
23. Enria DA, Barrera Oro JG, 2002. Junin virus vaccines. *Curr Top Microbiol Immunol 263:* 239–261.
24. Mahanty S, Bausch DG, Thomas RL, Goba A, Bah A, Peters CJ, Rollin PE, 2001. Low levels of interleukin-8 and interferon-inducible protein–10 in serum are associated with fatal infections in acute lassa fever. *J Infect Dis 183:* 1713–1721.
25. Stairs DB, Bayne LJ, Rhoades B, Vega ME, Waldron TJ, Kalabis J, Klein-Szanto A, Lee JS, Katz JP, Diehl JA, Reynolds AB, Vonderheide RH, Rustgi AK, 2011. Deletion of p120-catenin results in a tumor microenvironment with inflammation and cancer that establishes it as a tumor suppressor gene. *Cancer Cell 19:* 470–483.
26. Xiao K, Garner J, Buckley KM, Vincent PA, Chiasson CM, Dejana E, Faundez V, Kowalczyk AP, 2005. p120-Catenin regulates clathrin-dependent endocytosis of VE-cadherin. *Mol Biol Cell 16:* 5141–5151.
27. Herron CR, Lowery AM, Hollister PR, Reynolds AB, Vincent PA, 2011. p120 regulates endothelial permeability independently of its NH2 terminus and Rho binding. *Am J Physiol Heart Circ Physiol 300:* H36–H48.
28. Klavinskis LS, Oldstone MB, 1989. Lymphocytic choriomeningitis virus selectively alters differentiated but not housekeeping functions: block in expression of growth hormone gene is at the level of transcriptional initiation. *Virology 168:* 232–235.
29. Bureau JF, Le Goff S, Thomas D, Parlow AF, de la Torre JC, Homann D, Brahic M, Oldstone MB, 2001. Disruption of

differentiated functions during viral infection *in vivo*. V. Mapping of a locus involved in susceptibility of mice to growth hormone deficiency due to persistent lymphocytic choriomeningitis virus infection. *Virology 281:* 61–66.
30. Wright TJ, Leach L, Shaw PE, Jones P, 2002. Dynamics of vascular endothelial-cadherin and beta-catenin localization by vascular endothelial growth factor-induced angiogenesis in human umbilical vein cells. *Exp Cell Res 280:* 159–168.
31. Dejana E, Lampugnani MG, Martinez-Estrada O, Bazzoni G, 2000. The molecular organization of endothelial junctions and their functional role in vascular morphogenesis and permeability. *Int J Dev Biol 44:* 743–748.
32. Cheung LW, Leung PC, Wong AS, 2010. Cadherin switching and activation of p120 catenin signaling are mediators of gonadotropin-releasing hormone to promote tumor cell migration and invasion in ovarian cancer. *Oncogene 29:* 2427–2440.
33. Weis S, Shintani S, Weber A, Kirchmair R, Wood M, Cravens A, McSharry H, Iwakura A, Yoon Y-s, Himes N, Burstein D, Doukas J, Soll R, Losordo D, Cheresh D, 2004. Src blockade stabilizes a Flk/cadherin complex, reducing edema and tissue injury following myocardial infarction. *J Clin Invest 113:* 885–894.
34. Gorbunova EE, Gavrilovskaya IN, Pepini T, Mackow ER, 2011. VEGFR2 and Src kinase inhibitors suppress Andes virus-induced endothelial cell permeability. *J Virol 85:* 2296–2303.
35. Shrivastava-Ranjan P, Rollin PE, Spiropoulou CF, 2010. Andes virus disrupts the endothelial cell barrier by induction of vascular endothelial growth factor and downregulation of VE-cadherin. *J Virol 84:* 11227–11234.
36. Sathupan P, Khongphattanayothin A, Srisai J, Srikaew K, Poovorawan Y, 2007. The role of vascular endothelial growth factor leading to vascular leakage in children with dengue virus infection. *Ann Trop Paediatr 27:* 179–184.
37. Iyer S, Ferreri DM, DeCocco NC, Minnear FL, Vincent PA, 2004. VE-cadherin-p120 interaction is required for maintenance of endothelial barrier function. *Am J Physiol Lung Cell Mol Physiol 286:* L1143–L1153.
38. Maruo N, Morita I, Shirao M, Murota S, 1992. IL-6 increases endothelial permeability *in vitro*. *Endocrinology 131:* 710–714.
39. Arendt BK, Velazquez-Dones A, Tschumper RC, Howell KG, Ansell SM, Witzig TE, Jelinek DF, 2002. Interleukin 6 induces monocyte chemoattractant protein-1 expression in myeloma cells. *Leukemia 16:* 2142–2147.
40. Biswas P, Delfanti F, Bernasconi S, Mengozzi M, Cota M, Polentarutti N, Mantovani A, Lazzarin A, Sozzani S, Poli G, 1998. Interleukin-6 induces monocyte chemotactic protein-1 in peripheral blood mononuclear cells and in the U937 cell line. *Blood 91:* 258–265.
41. Clifton DR, Rydkina E, Huyck H, Pryhuber G, Freeman RS, Silverman DJ, Sahni SK, 2005. Expression and secretion of chemotactic cytokines IL-8 and MCP-1 by human endothelial cells after *Rickettsia rickettsii* infection: regulation by nuclear transcription factor NF-kappaB. *Int J Med Microbiol 295:* 267–278.
42. Lee YR, Liu MT, Lei HY, Liu CC, Wu JM, Tung YC, Lin YS, Yeh TM, Chen SH, Liu HS, 2006. MCP-1, a highly expressed chemokine in dengue haemorrhagic fever/dengue shock syndrome patients, may cause permeability change, possibly through reduced tight junctions of vascular endothelium cells. *J Gen Virol 87:* 3623–3630.
43. Tieu BC, Lee C, Sun H, Lejeune W, Recinos A 3rd, Ju X, Spratt H, Guo DC, Milewicz D, Tilton RG, Brasier AR, 2009. An adventitial IL-6/MCP1 amplification loop accelerates macrophage-mediated vascular inflammation leading to aortic dissection in mice. *J Clin Invest 119:* 3637–3651.
44. Rübe C, Wilfert F, Palm J, König J, Burdak-Rothkamm S, Liu L, Schuck A, Willich N, Rübe C, 2004. Irradiation induces a biphasic expression of pro-inflammatory cytokines in the lung. *Strahlenther Onkol 180:* 442–448.
45. Hebda PA, Piltcher OB, Swarts JD, Alper CM, Zeevi A, Doyle WJ, 2002. Cytokine profiles in a rat model of otitis media with effusion caused by eustachian tube obstruction with and without *Streptococcus pneumoniae* infection. *Laryngoscope 112:* 1657–1662.
46. Candurra NA, Lago MJ, Maskin L, Damonte EB, 1999. Involvement of the cytoskeleton in Junin virus multiplication. *J Gen Virol 80:* 147–156.
47. Martinez MG, Cordo SM, Candurra NA, 2008. Involvement of cytoskeleton in Junin virus entry. *Virus Res 138:* 17–25.
48. Pozner RG, Ure AE, Jaquenod de Giusti C, D'Atri LP, Italiano JE, Torres O, Romanowski V, Schattner M, Gomez RM, 2010. Junin virus infection of human hematopoietic progenitors impairs *in vitro* proplatelet formation and platelet release via a bystander effect involving type I IFN signaling. *PLoS Pathog 6:* e1000847.
49. Elsner B, Schwarz E, Mando OG, Maiztegui J, Vilches A, 1973. Pathology of 12 fatal cases of Argentine hemorrhagic fever. *Am J Trop Med Hyg 22:* 229–236.
50. Riviere Y, Gresser I, Guillon JC, Tovey MG, 1977. Inhibition by anti-interferon serum of lymphocytic choriomeningitis virus disease in suckling mice. *Proc Natl Acad Sci USA 74:* 2135–2139.
51. Emonet SF, Seregin AV, Yun NE, Poussard AL, Walker AG, de la Torre JC, Paessler S, 2011. Rescue from cloned cDNAs and *in vivo* characterization of recombinant pathogenic Romero and live-attenuated Candid #1 strains of Junin virus, the causative agent of Argentine hemorrhagic fever disease. *J Virol 85:* 1473–1483.
52. Arroyo AG, Iruela-Arispe ML, 2010. Extracellular matrix, inflammation, and the angiogenic response. *Cardiovasc Res 86:* 226–235.
53. Feldmann H, Klenk HD, 1996. Marburg and Ebola viruses. *Adv Virus Res 47:* 1–52.
54. Sundstrom JB, McMullan LK, Spiropoulou CF, Hooper WC, Ansari AA, Peters CJ, Rollin PE, 2001. Hantavirus infection induces the expression of RANTES and IP-10 without causing increased permeability in human lung microvascular endothelial cells. *J Virol 75:* 6070–6085.
55. Lee Y-R, Liu M-T, Lei H-Y, Liu C-C, Wu J-M, Tung Y-C, Lin Y-S, Yeh T-M, Chen S-H, Liu H-S, 2006. MCP-1, a highly expressed chemokine in dengue haemorrhagic fever/dengue shock syndrome patients, may cause permeability change, possibly through reduced tight junctions of vascular endothelium cells. *J Gen Virol 87:* 3623–3630.